Dzyaloshinskii-Moriya interaction at epitaxial ferromagnet/semiconductor interface

Shuto Kimura,[1] Michihiro Yamada,[2,3] Takumi Okuno,[1] Kentarou Sawano,[4] Kohei Hamaya,[2,3] and Kazuya Ando[1,5,6,*]

[1]*Department of Applied Physics and Physico-Informatics, Keio University, 3-14-1 Hiyoshi, Kohoku-ku, Yokohama 223-8522, Japan*

[2]*Center for Spintronics Research Network, Osaka University, 1-3 Machikaneyama, Toyonaka, Osaka 560-8531, Japan*

[3]*Spintronics Research Network Division, Institute for Open and Transdisciplinary Research Initiatives, Osaka University, 2-1 Yamadaoka, Suita, Osaka 565-0871, Japan*

[4]*Advanced Research Laboratories, Tokyo City University, 8-15-1 Todoroki, Setagaya-ku, Tokyo 158-0082, Japan*

[5]*Keio Institute of Pure and Applied Sciences, Keio University, 3-14-1 Hiyoshi, Kohoku-ku, Yokohama 223-8522, Japan*

[6]*Center for Spintronics Research Network, Keio University, 3-14-1 Hiyoshi, Kohoku-ku, Yokohama 223-8522, Japan*

(Received 18 May 2021; accepted 20 September 2023; published 28 September 2023)

We report a sizable Dzyaloshinskii-Moriya interaction (DMI) originating at an epitaxial Fe_3Si/Ge interface. Using spin-wave spectroscopy, we show that the magnitude of the interfacial DMI of the Heusler-ferromagnet/semiconductor hybrid structure is comparable to that of ferromagnet/Pt structures, despite the absence of heavy elements. We find that the observed DMI at the Fe_3Si/Ge interface is consistent with the prediction of an antisymmetric exchange interaction induced by the interfacial Bychkov-Rashba spin-orbit interaction. These results demonstrate that ferromagnet/semiconductor hybrid structures are a promising class of systems for chiral spintronics.

DOI: 10.1103/PhysRevB.108.094441

I. INTRODUCTION

The generation, stabilization, and manipulation of chiral spin structures, such as chiral Néel walls and magnetic skyrmions, provide the fundamental building blocks of chiral spintronics [1,2]. The formation of such nontrivial spin structures requires chiral symmetry breaking. In magnetic systems, the source of the chiral symmetry breaking is the antisymmetric exchange interaction that is referred to as the Dzyaloshinskii-Moriya interaction (DMI) [3,4]. The DMI originates from spin-orbit coupling (SOC) in magnetic systems with broken inversion symmetry, including noncentrosymmetric crystals or at interfaces of heterostructures. The latter is of particular recent interest due to their potential applications, such as data storage, brain-inspired architectures, and reservoir computing [5–9].

The search for material systems providing strong interfacial DMIs has been mainly focused on polycrystalline ferromagnetic-metal/heavy-metal (FM/HM) structures. The microscopic mechanism of the interfacial DMI in this system is well described by the Fert-Levy model, where the interaction between two neighboring magnetic ions with spins $\mathbf{S}_i$ and $\mathbf{S}_j$ is mediated by a third ion with strong SOC [10]. This model, as well as experimental observations, predicts that the strength of the DMI generally scales with the strength of the SOC of the adjacent HM layer. However, recent investigations have revealed that sizable interfacial DMIs can appear even in the absence of heavy elements. An example is the stabilization of chiral domain walls in a graphene/FM bilayer [11], where the magnitude of the DMI is comparable to that at interfaces with heavy metals [11,12]. Another example is sizable DMIs in conventional spintronic structures with oxide/FM interfaces, such as MgO/FM/Pt. In this system, a sizable DMI exists at the MgO/FM interface, as well as the FM/Pt interface [13]. The first-principles calculations have shown that, at the FM/Pt interface, the SOC energy source for the DMI is located within the interfacial Pt layer, consistent with the Fert-Levy mechanism. In contrast, at the MgO/FM interface, both the DMI and its SOC energy source are localized within the interfacial FM layer. These findings indicate that a mechanism different from the Fert-Levy mechanism gives rise to strong interfacial DMIs.

The source of the interfacial DMI without using heavy elements can be attributed to the Bychkov-Rashba SOC at the interface [14]. In the Rashba-type DMI model, the strength of the DMI is proportional to the Rashba parameter and exchange stiffness [14]. This picture is supported by the agreement between the experimentally obtained DMI values and theoretical values from the first-principles calculations [11]. The discovery of the direct link between the interfacial DMI and interfacial Rashba SOC offers promising opportunities for exploring the physics and technology of Rashba systems in chiral spintronics.

The recent progress in spintronics has revived interest in FM/semiconductor hybrid structures, which have been one of the key systems in establishing spintronic phenomena over the past two decades. For FM/semiconductor interfaces, the existence of robust Rashba SOC has been evidenced by the efficient charge-spin conversion and large unidirectional magnetoresistance [15–17]. Although these recent demonstrations suggest that a sizable DMI could also appear in FM/semiconductor heterostructures, experimental evidence of its existence is scarce.

*ando@appi.keio.ac.jp

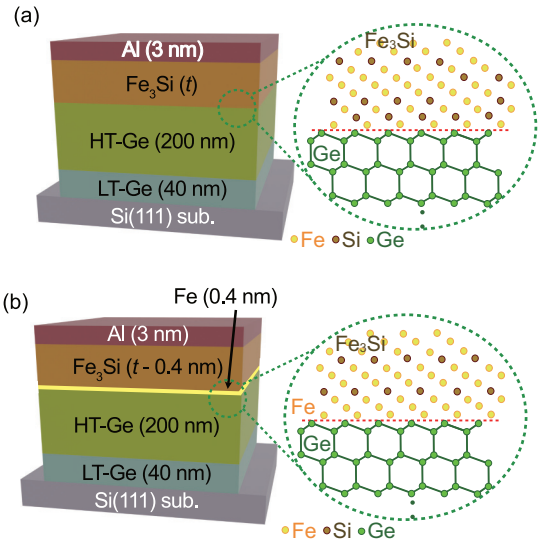

FIG. 1. Schematic illustrations of the (a) unterminated $Al/Fe_3Si(t)/Ge$ film and (b) Fe-terminated $Al/Fe_3Si(t-0.4\ nm)/Fe(0.4\ nm)/Ge$ film.

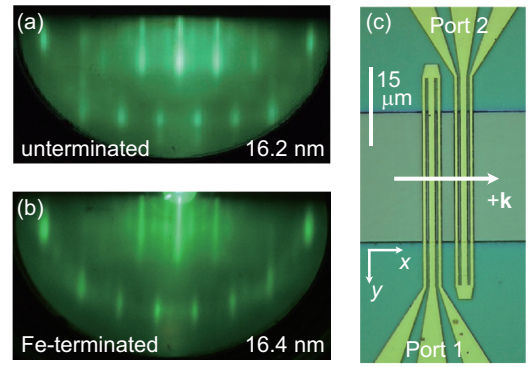

FIG. 2. RHEED patterns from the surface of the (a) unterminated $Fe_3Si(16.2\ nm)$ and (b) Fe-terminated $Fe_3Si(16.4\ nm)$ on Ge-on-Si(111). (c) An optical image of the device with electrical connections, labeled as "Port 1" and "Port 2." The spin wave excited by the antenna "Port 1" is represented by the wave vector $+\mathbf{k}$.

In this paper, we report sizable DMIs at epitaxial Fe_3Si/Ge interfaces, where Fe_3Si is a ferromagnetic Heusler alloy [18]. Among semiconductors, Ge has attracted broad interest because of its high mobility, long spin lifetime, and compatibility with the Si platform [19]. Although the bulk SOC of Ge is weak enough to result in a long spin diffusion length, the large Rashba energy splitting of the subsurface states has been shown to give rise to sizable unidirectional Rashba magnetoresistance [17]. Furthermore, the Rashba SOC can be greatly enhanced at the metal/Ge interfaces [20–22]. In this work, by measuring propagating spin-wave spectroscopy, we find that the magnitude of the DMI at the Fe_3Si/Ge interface is comparable to that in FM/HM systems, despite the absence of heavy elements. We show that the observed DMI can be attributed to the Rashba-type DMI. Our results indicate that epitaxial FM/semiconductor interfaces can be a promising platform for chiral spintronics.

II. EXPERIMENTAL METHODS

To investigate the DMI at the Fe_3Si/Ge interface, we fabricated two series of samples on Si(111) substrates by molecular beam epitaxy (MBE): (i) $Al\,(3\,nm)/Fe_3Si(t)/Ge(240\ nm)$ [unterminated $Al/Fe_3Si/Ge$, Fig. 1(a)] and (ii) $Al(3\ nm)/Fe_3Si(t-0.4\ nm)/Fe(0.4\ nm)/Ge\,(240\ nm)$ [Fe-terminated $Al/Fe_3Si/Ge$, Fig. 1(b)] films, where the numbers in parentheses represent the thickness. First, the undoped Ge-on-Si(111) was fabricated using the two-step growth method, where a low-temperature-grown Ge (LT-Ge) film with a thickness of 40 nm and a high-temperature-grown Ge (HT-Ge) film ($\sim$0.1 Ω cm) with a thickness of 200 nm were subsequently grown on a Si(111) substrate ($\sim$1000 Ω cm) at 350 and 700 °C, respectively. The Ge epilayer grown on the Si(111) substrate shows *p*-type conduction and (111) crystal orientation [23]. Then, using low-temperature MBE techniques, the Heusler alloy, Fe_3Si with a thickness of t, was formed on the Ge film at a growth temperature below 80 °C. The detailed growth conditions are described in our previous report [19]. Here, although the ideal Fe_3Si layer has a periodical structure consisting of three Fe layers and one Si layer, the Fe_3Si layer near the Fe_3Si/Ge interface includes a disordered structure in the unterminated $Al/Fe_3Si/Ge$ film [24]. Since the interfacial DMI can be sensitive to the atomic arrangements at the interface, we controlled the Fe_3Si/Ge interface by introducing the Fe termination layer in the Fe-terminated $Al/Fe_3Si/Fe/Ge$ [see Figs. 1(a) and 1(b)]. Finally, a 3-nm-thick Al capping layer was deposited on the Fe_3Si layer below 50 °C to avoid natural oxidation of the film and interdiffusion between the capping layer and Fe_3Si layer.

We show representative reflection high-energy electron diffraction (RHEED) patterns for the surface of the Fe_3Si layer of the unterminated Fe_3Si/Ge and the Fe-terminated Fe_3Si/Ge in Figs. 2(a) and 2(b), respectively. The results clearly exhibit a symmetrical streak, indicating good epitaxial growth of the Fe_3Si layer on the Ge-on-Si(111). For all films used in this study, we measured magnetic hysteresis loops, which show that the variation of the saturation magnetization M_s of the Fe_3Si layers with different thicknesses t is within 5% of the average value. This result confirms that M_s of the Fe_3Si layer is independent of the thickness t, indicating the epitaxial growth of the Fe_3Si/Ge interfaces without reaction layers, as shown in Ref. [19]; if reaction layers are formed at the interfaces of Fe_3Si/Ge and Al/Fe_3Si, the value of M_s decreases because the diffused Ge atoms substitute for magnetic Fe sites.

For the propagating spin-wave spectroscopy, the films were patterned into 30-μm-wide strips, and the surface were covered by a 50-nm-thick SiO_2 insulator film. We fabricated a pair of meander-shaped microwave antennas of Au(200 nm)/Ti(3 nm) on top of the strip using electron beam lithography, as shown in Fig. 2(c). The antennas are designed to excite spin waves with a wave number of $k = 1.7\ \mu m^{-1}$ effectively; the center-to-center distance between the antennas is $l = 7.4$ μm, and the widths of a signal line and two ground lines are 1.4 and 0.7 μm, respectively [25]. For the devices, we measured the scattering parameters S_{ij}, where i and j (=1, 2) correspond to the receiving and emitting antenna, using a vec-

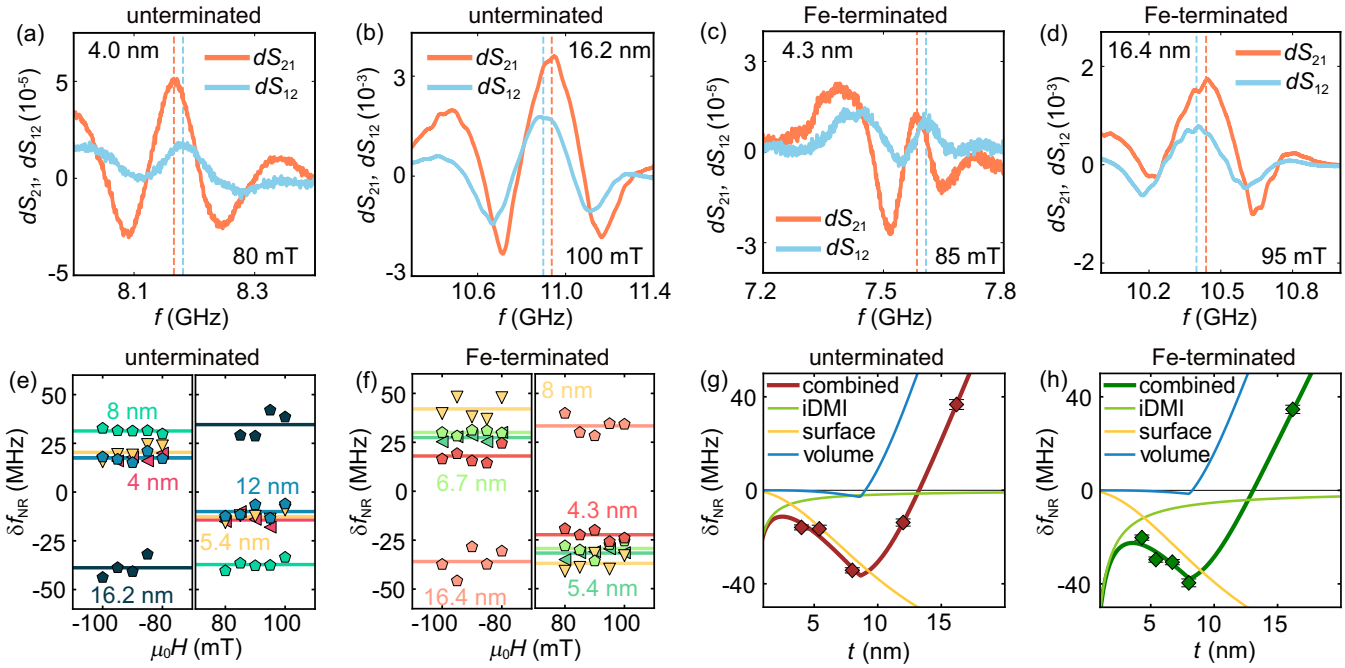

FIG. 3. Propagating spin-wave spectra dS_{21} and dS_{12} for the unterminated Al/$Fe_3Si(t)$/Ge with (a) $t = 4.0$ nm at $\mu_0 H = 80$ mT and (b) $t = 16.2$ nm at $\mu_0 H = 100$ mT. The orange and blue dotted lines represent the MSSW resonance frequencies at $k = +1.7$ and -1.7 μm^{-1}, respectively. dS_{21} and dS_{12} for the Fe-terminated Al/$Fe_3Si(t-0.4)$/Fe(0.4)/Ge with (c) $t = 4.3$ nm at $\mu_0 H = 85$ mT and (d) $t = 16.4$ nm at $\mu_0 H = 95$ mT. Magnetic field H dependence of the frequency difference δf_{NR} for the (e) unterminated Al/$Fe_3Si(t)$/Ge and (f) Fe-terminated Al/$Fe_3Si(t-0.4)$/Fe(0.4)/Ge films with different t. The plots of each color represent experimental data. The solid lines represent the average value for each thickness data. Fe_3Si-thickness t dependence of δf_{NR} for the (g) unterminated Al/$Fe_3Si(t)$/Ge and (h) Fe-terminated Al/$Fe_3Si(t-0.4)$/Fe(0.4)/Ge. The diamond-shaped symbols are the experimental data. Light green, yellow, and blue lines are the frequency nonreciprocity induced by the iDMI, interfacial PMA (surface), and bulk PMA (volume), respectively. We used $\gamma = 1.94 \times 10^{11}$ s^{-1} T^{-1} for the fitting. The standard error of the determined values of δf_{NR} is represented by the error bars, which were derived from δf_{NR} measured at various H.

tor network analyzer (VNA) by applying an external magnetic field H at room temperature. To excite magnetostatic surface waves (MSSWs) with the wave vector perpendicular to the magnetic field, H was applied along the y axis [see Fig. 2(c)].

III. RESULTS AND DISCUSSION

Figures 3(a)–3(d) show the transmission spectra for the unterminated and Fe-terminated Al/Fe_3Si/Ge films. Here, the frequency response of the transmission at the magnetic field H is defined as $dS_{ij} = S_{ij}(H) - S_{ij}(H_{ref})$, where $S_{ij}(H_{ref})$ is the scattering parameter at a reference magnetic field $\mu_0 H_{ref} = 250$ mT in which the resonance peaks are located out of the measured frequency range. In Figs. 3(a)–3(d), dS_{21} and dS_{12} correspond to the waves with $k < 0$ and $k > 0$, respectively. Since $l \times k \sim 4\pi$, the orange and blue dotted lines represent the MSSW resonance frequencies at $k = +1.7$ μm^{-1} and $k = -1.7$ μm^{-1}, respectively [26]. We define the frequency shift δf_{NR} as the difference between the MSSW resonance frequencies of the counterpropagating spin waves. The resonance frequencies were determined by fitting the measured signals around their peaks using a Lorentz function.

In Figs. 3(e) and 3(f), we show δf_{NR} measured at different magnetic fields H for the unterminated Al/Fe_3Si/Ge and Fe-terminated Al/Fe_3Si/Ge devices, respectively. Figures 3(e) and 3(f) show that the magnitude of δf_{NR} is independent of the field strength, while the sign of δf_{NR} is reversed by reversing the field direction, consistent with the prediction of the frequency shift of the MSSWs induced by the DMI. This result also shows that the magnitude and sign of δf_{NR} depend on the thickness t of the Fe_3Si layer.

We show the t dependence of δf_{NR} for the unterminated Al/Fe_3Si/Ge and Fe-terminated Al/Fe_3Si/Ge devices in Figs. 3(g) and 3(h), respectively. The t-dependent change in δf_{NR} arises from three contributions: (i) the interfacial DMI (iDMI), (ii) the asymmetry in the surface magnetic anisotropy, and (iii) the nonuniformity of the bulk magnetic anisotropy [27]. First, the frequency shift due to the iDMI is proportional to $1/t$. The reason for this is that due to the interfacial origin of the DMI, the volumetric DMI constant D_{DMI} is proportional to $1/t$, $D_{DMI} = D_s/t$, where D_s is the thickness-independent DMI constant [28]. Second, the spin-wave nonreciprocity also arises from the difference between the interfacial perpendicular magnetic anisotropy (PMA) energy density at the bottom K_s^{bot} and the top K_s^{top} interfaces, $\delta K_s = K_s^{bot} - K_s^{top}$ [29,30]. Third, a recent study has shown that the nonuniformity of the bulk magnetic anisotropy across the film can also result in spin-wave nonreciprocity [27]. The frequency shift taking into account the three contributions is expressed as [27]

$$\delta f_{NR} = \frac{2\gamma D_s}{\pi M_s t} k + \frac{\gamma \mu_0 M_s}{2\pi} 2Q\delta \frac{\Omega_{0,z} - \Omega_{1,z}}{\Omega_0^2 - \Omega_1^2}, \quad (1)$$

TABLE I. Summary of the magnitude of the thickness-independent DMI parameter $|D_s|$ for the unterminated Al/Fe_3Si/Ge and Fe-terminated Al/Fe_3Si/Ge, as well as conventional FM/Pt systems with Fe-based ferromagnetic layers.

Structure	$\lvert D_s\rvert$ (pJ/m)	Ref.
Unterminated Al/Fe_3Si/Ge	0.08 ± 0.05	This work
Fe-terminated Al/Fe_3Si/Ge	0.21 ± 0.06	This work
Ti/Py/Pt	0.25	[30]
SiN/$Ni_{80}Fe_{20}$/Pt	0.15–0.33	[28]
MgO/$Co_{20}Fe_{60}B_{20}$/Pt	0.97	[32]

where γ is the gyromagnetic ratio. The parameters Q, δ, $\Omega_{0,z}$, $\Omega_{1,z}$, Ω_0, and Ω_1 are defined in the literature [27]. In Eq. (1), the contribution (iii) is modeled as a difference in the bulk magnetic anisotropy between the below and above critical thickness t_{cr} in the FM layer, where the out-of-plane magnetic anisotropy K is assumed to be $K = K_s/t + K_{v,0}$ for $t \leqslant t_{cr}$ and $K = K_s/t + K_{v,0} + K_{v,1}(t - t_{cr})/t$ for $t > t_{cr}$, where $K_s = K_s^{bot} + K_s^{top}$ is the total interfacial anisotropy, $K_{v,0}$ is the bulk magnetic anisotropy of the FM layer below t_{cr}, and $K_{v,1}$ is the difference in the bulk magnetic anisotropy between above and below t_{cr} [27]. We fit the t dependence of δf_{NR} by using Eq. (1), as shown in Figs. 3(g) and 3(h). From the fitting, we obtained $\delta K_s = -1.1$ mJ/m^2 for both the unterminated and Fe-terminated Al/Fe_3Si/Ge. This result suggests that δK_s is insensitive to the Fe termination, implying that the interfacial PMA can be primarily attributed to the Al/Fe_3Si interface, where the natural oxidation of the Al layer can enhance the interfacial PMA [31], rather than the lattice-matched Fe_3Si/Ge interface. We also obtained $K_{v,1} = -0.3$ mJ/m^3, and $t_{cr} = 8.6$ nm for the unterminated Al/Fe_3Si/Ge and $K_{v,1} = -0.3$ mJ/m^3, and $t_{cr} = 8.1$ nm for the Fe-terminated Al/Fe_3Si/Ge.

In Table I, we show the thickness-independent DMI constant D_s, extracted from the t dependence of δf_{NR} using Eq. (1). Table I shows that the D_s of the Fe-terminated Al/Fe_3Si/Ge is more than twice that of the unterminated Al/Fe_3Si/Ge. This result demonstrates that the DMI at the Fe_3Si/Ge interface is quite sensitive to the atomic arrangements at the interface, revealing the crucial role of atomic-level engineering in controlling the iDMI at FM/semiconductor interfaces. To compare the magnitude of the DMI at the epitaxial Fe_3Si/Ge interfaces with that of the conventional FM/HM systems, we also list the DMI constant for systems with Fe-based ferromagnetic layers in Table I. This result shows that the strength of the DMI at the Fe_3Si/Ge interfaces can be comparable to that at the FM/Pt interfaces, despite the fact that the atomic SOC of Ge is much weaker than that of Pt [33]. This finding suggests that the physical mechanism governing the DMI at the Fe_3Si/Ge interfaces is different from that at the FM/Pt interfaces, captured by the Fert-Levy model.

The sizable DMI at the Fe_3Si/Ge interface can be attributed to the Rashba-type DMI [14,34]. In the model of the Rashba-type DMI, the DMI strength for two-dimensional (2D) Rashba ferromagnets is expressed as $D_{2D} = 2k_R A$, where $k_R = 2\alpha_R m_e/\hbar^2$ [14]. Here, α_R is the Rashba parameter, m_e is the effective electron mass, and $\hbar$ is the reduced Planck constant. Although first-principles calculations are necessary to fully understand the microscopic mechanism of the interfacial DMI, we roughly estimate the Rashba parameter at the Fe_3Si/Ge interface from the extracted value of D_s based on this simple model. Under the assumption that only the first Fe_3Si layer at the Ge interface contributes to the DMI, the DMI strength at the interface layer D_{int} can be estimated as $D_{int} = D_s/t_{int}$, where t_{int} is the thickness of the interface layer [28]. At the Fe_3Si/Ge(111) interface, the nearest interatomic distance between Ge and Fe is 0.15 nm, indicating that the interlayer distance between Ge and Fe is about 0.1 nm [24]. Using $D_{int} = 2k_R A$ and assuming that t_{int} corresponds to the distance between the Ge and Fe layers at the Fe_3Si/Ge interface, $t_{int} \approx 0.1$ nm, we obtain $k_R = 1.3 \times 10^8$ m^{-1} for the measured value of $|D_s| = 0.21$ pJ/m (see Table I). The corresponding Rashba parameter when m_e is assumed to be the free-electron mass is $\alpha_R = 50$ meV Å. This value is consistent with the strength of the Rashba SOC at a Fe/Ge(111) interface obtained from first-principles electronic band structure calculations based on the density functional theory [35], supporting that the DMI at the Fe_3Si/Ge interface is dominated by the interfacial Rashba SOC. The existence of the Rashba-type DMI has recently been suggested by experiments and calculations for oxide/oxide interfaces [36–39], FM/oxide interfaces [13,40], and FM/2D-material interfaces [11,12]. The observation of a sizable Rashba-type DMI at the Fe_3Si/Ge interface puts FM/semiconductor hybrid structures into the family of systems for chiral spintronics based on the Rashba SOC.

The observation of a sizable DMI at the Fe_3Si/Ge interface suggests that epitaxial FM/semiconductor heterostructures are a promising platform for a variety of interfacial SOC-induced phenomena. We note that the estimated value of $\alpha_R = 50$ meV Å at the Fe_3Si/Ge interface in the Fe-terminated samples is comparable to $\alpha_R = 82.6$ meV Å at a graphene/Co interface, which shows a significant DMI [11]. The Rashba parameter is also comparable to that of the archetypal systems which have been central in establishing the physics of transport phenomena induced by the Rashba SOC, such as $\alpha_R = 67$ meV Å in an InGaAs/InAlAs heterostructure [41] and $\alpha_R = 30$ meV Å at a $LaAlO_3/SrTiO_3$ interface [42].

IV. CONCLUSIONS

We have investigated the DMI in the epitaxial Fe_3Si/Ge structures. Using the propagating spin-wave spectroscopy, we found that a sizable DMI exists at the Fe_3Si/Ge interface, despite the absence of heavy elements. While first-principles calculations are necessary for a comprehensive understanding of the DMI, we have shown that the observed interfacial DMI is consistent with the prediction of a chiral magnetic exchange interaction originating from the interfacial Rashba SOC.

The DMI was first described by a phenomenological thermodynamic theory [3]. The recent progress in spintronics has shed new light on this interaction, and it is now fundamental to understand the microscopic origin of the interfacial DMI. This clearly requires the experimental determination of intrinsic DMI parameters, free from extrinsic effects at the interface. However, experimental studies on the interfacial DMI have mainly focused on polycrystalline oxide/FM/HM structures without well-defined interfaces, despite the fact that interface

intermixing, interface roughness, dead layers, and proximity effects are all known to affect the interfacial DMI. The present work, based on the epitaxial Fe_3Si/Ge structures with controlled interfaces, has revealed that the DMI is highly sensitive to the atomic disorders at the interface. This finding demonstrates the crucial role of atomic-scale engineering of interfaces for controlling, enhancing, and understanding the interfacial DMI, which will be essential for the development of chiral spintronics.

ACKNOWLEDGMENTS

This work was supported by JSPS KAKENHI (Grants No. 20H00337, No. 22H04964, No. 19H05616, and No. 19H00864), JST FOREST Program (Grant No. JPMJFR2032), and Spintronics Research Network of Japan (Spin-RNJ).

S.K., M.Y., and T.O. contributed equally to this work.

[1] N. Nagaosa and Y. Tokura, Topological properties and dynamics of magnetic skyrmions, Nat. Nanotechnol. **8**, 899 (2013).

[2] S.-H. Yang, R. Naaman, Y. Paltiel, and S. S. Parkin, Chiral spintronics, Nat. Rev. Phys. **3**, 328 (2021).

[3] I. Dzyaloshinsky, A thermodynamic theory of "weak" ferromagnetism of antiferromagnetics, J. Phys. Chem. Solids **4**, 241 (1958).

[4] T. Moriya, Anisotropic superexchange interaction and weak ferromagnetism, Phys. Rev. **120**, 91 (1960).

[5] A. Fert, V. Cros, and J. Sampaio, Skyrmions on the track, Nat. Nanotechnol. **8**, 152 (2013).

[6] J. Sampaio, V. Cros, S. Rohart, A. Thiaville, and A. Fert, Nucleation, stability and current-induced motion of isolated magnetic skyrmions in nanostructures, Nat. Nanotechnol. **8**, 839 (2013).

[7] S. Parkin and S.-H. Yang, Memory on the racetrack, Nat. Nanotechnol. **10**, 195 (2015).

[8] S. Emori, U. Bauer, S.-M. Ahn, E. Martinez, and G. S. Beach, Current-driven dynamics of chiral ferromagnetic domain walls, Nat. Mater. **12**, 611 (2013).

[9] D. Prychynenko, M. Sitte, K. Litzius, B. Krüger, G. Bourianoff, M. Kläui, J. Sinova, and K. Everschor-Sitte, Magnetic Skyrmion as a Nonlinear Resistive Element: A Potential Building Block for Reservoir Computing, Phys. Rev. Appl. **9**, 014034 (2018).

[10] A. Fert and P. M. Levy, Role of Anisotropic Exchange Interactions in Determining the Properties of Spin-Glasses, Phys. Rev. Lett. **44**, 1538 (1980).

[11] H. Yang, G. Chen, A. A. C. Cotta, A. T. N'Diaye, S. A. Nikolaev, E. A. Soares, W. A. A. Macedo, K. Liu, A. K. Schmid, A. Fert, and M. Chshiev, Significant Dzyaloshinskii–Moriya interaction at graphene–ferromagnet interfaces due to the Rashba effect, Nat. Mater. **17**, 605 (2018).

[12] F. Ajejas, A. Gudín, R. Guerrero, A. Anadón Barcelona, J. M. Diez, L. de Melo Costa, P. Olleros, M. A. Niño, S. Pizzini, J. Vogel, M. Valvidares, P. Gargiani, M. Cabero, M. Varela, J. Camarero, R. Miranda, and P. Perna, Unraveling Dzyaloshinskii-Moriya interaction and chiral nature of graphene/cobalt interface, Nano Lett. **18**, 5364 (2018).

[13] H. Yang, O. Boulle, V. Cros, A. Fert, and M. Chshiev, Controlling Dzyaloshinskii-Moriya interaction via chirality dependent atomic-layer stacking, insulator capping and electric field, Sci. Rep. **8**, 12356 (2018).

[14] K.-W. Kim, H.-W. Lee, K.-J. Lee, and M. D. Stiles, Chirality from Interfacial Spin-Orbit Coupling Effects in Magnetic Bilayers, Phys. Rev. Lett. **111**, 216601 (2013).

[15] L. Chen, M. Decker, M. Kronseder, R. Islinger, M. Gmitra, D. Schuh, D. Bougeard, J. Fabian, D. Weiss, and C. H. Back, Robust spin-orbit torque and spin-galvanic effect at the Fe/GaAs (001) interface at room temperature, Nat. Commun. **7**, 13802 (2016).

[16] L. Chen, M. Gmitra, M. Vogel, R. Islinger, M. Kronseder, D. Schuh, D. Bougeard, J. Fabian, D. Weiss, and C. Back, Electric-field control of interfacial spin–orbit fields, Nat. Electron. **1**, 350 (2018).

[17] T. Guillet, C. Zucchetti, Q. Barbedienne, A. Marty, G. Isella, L. Cagnon, C. Vergnaud, H. Jaffrès, N. Reyren, J.-M. George, A. Fert, and M. Jamet, Observation of Large Unidirectional Rashba Magnetoresistance in Ge(111), Phys. Rev. Lett. **124**, 027201 (2020).

[18] A. Ionescu, C. A. F. Vaz, T. Trypiniotis, C. M. Gürtler, H. García-Miquel, J. A. C. Bland, M. E. Vickers, R. M. Dalgliesh, S. Langridge, Y. Bugoslavsky, Y. Miyoshi, L. F. Cohen, and K. R. A. Ziebeck, Structural, magnetic, electronic, and spin transport properties of epitaxial Fe_3Si/GaAs(001), Phys. Rev. B **71**, 094401 (2005).

[19] K. Hamaya, Y. Fujita, M. Yamada, M. Kawano, S. Yamada, and K. Sawano, Spin transport and relaxation in germanium, J. Phys. D: Appl. Phys. **51**, 393001 (2018).

[20] Y. Ohtsubo, S. Hatta, K. Yaji, H. Okuyama, K. Miyamoto, T. Okuda, A. Kimura, H. Namatame, M. Taniguchi, and T. Aruga, Spin-polarized semiconductor surface states localized in subsurface layers, Phys. Rev. B **82**, 201307(R) (2010).

[21] Y. Ohtsubo, K. Yaji, S. Hatta, H. Okuyama, and T. Aruga, Two-dimensional states localized in subsurface layers of Ge(111), Phys. Rev. B **88**, 245310 (2013).

[22] C.-H. Lin, T.-R. Chang, R.-Y. Liu, C.-M. Cheng, K.-D. Tsuei, H.-T. Jeng, C.-Y. Mou, I. Matsuda, and S.-J. Tang, Rashba effect within the space–charge layer of a semiconductor, New J. Phys. **16**, 045003 (2014).

[23] K. Sawano, Y. Hoshi, S. Kubo, K. Arimoto, J. Yamanaka, K. Nakagawa, K. Hamaya, M. Miyao, and Y. Shiraki, Structural and electrical properties of Ge(111) films grown on Si(111) substrates and application to Ge(111)-on-insulator, Thin Solid Films **613**, 24 (2016).

[24] S. Yamada, J. Sagar, S. Honda, L. Lari, G. Takemoto, H. Itoh, A. Hirohata, K. Mibu, M. Miyao, and K. Hamaya, Room-temperature structural ordering of a Heusler compound Fe_3Si, Phys. Rev. B **86**, 174406 (2012).

[25] V. Vlaminck and M. Bailleul, Spin-wave transduction at the submicrometer scale: Experiment and modeling, Phys. Rev. B **81**, 014425 (2010).

[26] K. Yamanoi, S. Yakata, T. Kimura, and T. Manago, Spin wave excitation and propagation properties in a permalloy film, Jpn. J. Appl. Phys. **52**, 083001 (2013).

[27] J. Lucassen, C. F. Schippers, M. A. Verheijen, P. Fritsch, E. J. Geluk, B. Barcones, R. A. Duine, S. Wurmehl, H. J. M. Swagten, B. Koopmans, and R. Lavrijsen, Extraction of Dzyaloshinskii-Moriya interaction from propagating spin waves, Phys. Rev. B **101**, 064432 (2020).

[28] H. T. Nembach, J. M. Shaw, M. Weiler, E. Jué, and T. J. Silva, Linear relation between Heisenberg exchange and interfacial Dzyaloshinskii–Moriya interaction in metal films, Nat. Phys. **11**, 825 (2015).

[29] O. Gladii, M. Haidar, Y. Henry, M. Kostylev, and M. Bailleul, Frequency nonreciprocity of surface spin wave in permalloy thin films, Phys. Rev. B **93**, 054430 (2016).

[30] O. Gladii, M. Collet, Y. Henry, J.-V. Kim, A. Anane, and M. Bailleul, Determining Key Spin-Orbitronic Parameters via Propagating Spin Waves, Phys. Rev. Appl. **13**, 014016 (2020).

[31] B. Dieny and M. Chshiev, Perpendicular magnetic anisotropy at transition metal/oxide interfaces and applications, Rev. Mod. Phys. **89**, 025008 (2017).

[32] X. Ma, G. Yu, C. Tang, X. Li, C. He, J. Shi, K. L. Wang, and X. Li, Interfacial Dzyaloshinskii-Moriya Interaction: Effect of 5*d* Band Filling and Correlation with Spin Mixing Conductance, Phys. Rev. Lett. **120**, 157204 (2018).

[33] M. Montalti, A. Credi, L. Prodi, and M. T. Gandolfi, *Handbook of Photochemistry* (CRC Press, Boca Raton, FL, 2006).

[34] A. Kundu and S. Zhang, Dzyaloshinskii-Moriya interaction mediated by spin-polarized band with Rashba spin-orbit coupling, Phys. Rev. B **92**, 094434 (2015).

[35] S. Oyarzún, A. K. Nandy, F. Rortais, J. C. Rojas-Sánchez, M. T. Dau, P. Noël, P. Laczkowski, S. Pouget, H. Okuno, L. Vila, C. Vergnaud, C. Beigné, A. Marty, J. P. Attané, S. Gambarelli, J. M. George, H. Jaffrès, S. Blügel, and M. Jamet, Evidence for spin-to-charge conversion by Rashba coupling in metallic states at the Fe/Ge(111) interface, Nat. Commun. **7**, 13857 (2016).

[36] C. O. Avci, E. Rosenberg, L. Caretta, F. Büttner, M. Mann, C. Marcus, D. Bono, C. A. Ross, and G. S. Beach, Interface-driven chiral magnetism and current-driven domain walls in insulating magnetic garnets, Nat. Nanotechnol. **14**, 561 (2019).

[37] S. Ding, A. Ross, R. Lebrun, S. Becker, K. Lee, I. Boventer, S. Das, Y. Kurokawa, S. Gupta, J. Yang, G. Jakob, and M. Kläui, Interfacial Dzyaloshinskii-Moriya interaction and chiral magnetic textures in a ferrimagnetic insulator, Phys. Rev. B **100**, 100406(R) (2019).

[38] S. Vélez, J. Schaab, M. S. Wörnle, M. Müller, E. Gradauskaite, P. Welter, C. Gutgsell, C. Nistor, C. L. Degen, M. Trassin, M. Fiebig, and P. Gambardella, High-speed domain wall racetracks in a magnetic insulator, Nat. Commun. **10**, 4750 (2019).

[39] S. Banerjee, O. Erten, and M. Randeria, Ferromagnetic exchange, spin-orbit coupling and spiral magnetism at the $LaAlO_3/SrTiO_3$ interface, Nat. Phys. **9**, 626 (2013).

[40] T. Srivastava, M. Schott, R. Juge, V. Křižáková, M. Belmeguenai, Y. Roussigné, A. Bernand-Mantel, L. Ranno, S. Pizzini, S.-M. Chérif, A. Stashkevich, S. Auffret, O. Boulle, G. Gaudin, M. Chshiev, C. Baraduc, and H. Béa, Large-voltage tuning of Dzyaloshinskii–Moriya interactions: A route toward dynamic control of skyrmion chirality, Nano Lett. **18**, 4871 (2018).

[41] J. Nitta, T. Akazaki, H. Takayanagi, and T. Enoki, Gate Control of Spin-Orbit Interaction in an Inverted $In_{0.53}Ga_{0.47}As/In_{0.52}Al_{0.48}As$ Heterostructure, Phys. Rev. Lett. **78**, 1335 (1997).

[42] E. Lesne, Y. Fu, S. Oyarzun, J. C. Rojas-Sánchez, D. C. Vaz, H. Naganuma, G. Sicoli, J. P. Attané, M. Jamet, E. Jacquet, J. M. George, A. Barthélémy, H. Jaffrès, A. Fert, M. Bibes, and L. Vila, Highly efficient and tunable spin-to-charge conversion through Rashba coupling at oxide interfaces, Nat. Mater. **15**, 1261 (2016).